DMD Fast Forward. Published on July 24, 2012 as doi:10.1124/dmd.112.046748

Regulation of PXR function and *UGT1A1* gene expression by post-translational modification of PXR protein

Junko Sugatani, Takahiro Uchida, Masatoshi Kurosawa, Masahiko Yamaguchi, Yasuhiro Yamazaki, Akira Ikari, and Masao Miwa

Department of Pharmaco-Biochemistry and Global Center of Excellence for Innovation in Human Health Sciences (Global COE), School of Pharmaceutical Sciences, University of Shizuoka, Japan (J.S., T.U., M.K., M.Y., Y.Y., A.I., M.M.)

Running title: Post-translational modification of PXR protein

Address correspondence and reprint to Dr. Junko Sugatani,

Department of Pharmaco-Biochemistry, School of Pharmaceutical Sciences, University of Shizuoka, 52-1 Yada, Suruga-ku, Shizuoka 422-8526, Japan.

Phone: (81)-54-264-5779; Fax: (81)-54-264-5773;

E-mail: sugatani@u-shizuoka-ken.ac.jp

Text pages: 34 pages

Number of Figures: 10 Figures

References: 36 References

Number of words: 250 words in Abstract

741 words in Introduction

1499 words in Discussion

ABBREVIATIONS: ACK, acetylated lysine; AhR, aryl hydrocarbon receptor; ARNT, aryl hydrocarbon nuclear translocator; B[a]P, benzo[a]pyrene; CAR, constitutive androstane receptor; hsp90, heat shock protein 90; CCRP, cytoplasmic CAR retention protein; CDK, cyclin-dependent kinase; DBD, DNA-binding domain; HDAC, histone deacetylase; GFP, green fluorescent protein; GST, glutathione S-transferase; LBD, ligand-binding domain; P450, cytochrome P450; PCR, polymerase chain reaction; pGL4-tk, pGL4-tk-firefly luciferase vector; PXR, pregnane X receptor; RIF, rifampicin; RXR, retinoid X receptor; siRNA, small interfering RNA; SRC, steroid receptor coactivator; tk, thymidine kinase promoter; UGT, UDP-glucuronosyltransferase; YFP, yellow fluorescent protein.

DMD Fast Forward. Published on July 24, 2012 as DOI: 10.1124/dmd.112.046748
This article has not been copyedited and formatted. The final version may differ from this version.

Abstract

Human UDP-glucuronosyltransferase (UGT) 1A1 is a critical enzyme responsible for detoxification and metabolism of endogenous and exogenous lipophilic compounds such as bilirubin. The present study shows how CDK inhibitor roscovitine stimulated the expression of UGT1A1 in HepG2 cells. Pregnane X receptor (PXR)-mediated transactivation of *UGT1A1* reporter gene was more prominently enhanced by roscovitine, compared with the basal-, constitutive androstane receptor-, and aryl hydrocarbon receptor-mediated activities. W e determined the regulatory mechanism of *UGT1A1* expression through PXR's stimulation by roscovitine. W hile phosphomimetic mutations at T290 and T408 retained the PXR protein in cytoplasm and attenuated the induction of UGT1A1 expression by both roscovitine and rifampicin, a mutation at S350 specifically reduced the activity of PXR induced by roscovitine. Immunoprecipitation analysis revealed that the T290D but not T408D mutant protein remained in cytoplasm by forming a complex with heat shock protein 90 and cytoplasmic CAR retention protein, whereas treatment with proteasome inhibitor MG-132 accumulated the T408D mutant protein in cytoplasm. Transfection with anti-CDK2 siRNA but not anti-CDK1 or CDK5 siRNA led to enhanced expression of UGT1A1. S350D YFP-PXR fusion protein could translocate from cytoplasm to nucleus similar to the wild-type protein, but was detected as an acetylated protein, whose binding with retinoid X receptor and histone deacetylase was impaired. Co-transfection with co-activator SRC-2 but not SRC-1 partly recovered its PXR activity. These results indicate that roscovitine stimulated the expression of UGT1A1 by inhibiting CDK2, which phosphorylated PXR at S350 to suppress binding with RXR and co-activator and maintain the acetylation of PXR protein.

DMD Fast Forward. Published on July 24, 2012 as DOI: 10.1124/dmd.112.046748
This article has not been copyedited and formatted. The final version may differ from this version.

Introduction

The constitutive androstane receptor (CAR, NR1I3) and pregnane X receptor (PXR, NR1I2) were originally characterized as nuclear hormone receptors that interact with a subset of retinoic acid response elements and have been recognized as xenobiotic-sensing nuclear receptors that transcriptionally regulate the expression of genes of phase I, II, and III metabolic enzymes and transporters involved in the metabolism and elimination of endogenous and exogenous substances such as bilirubin, steroid hormones, and xenobiotics (Timsit and Negishi, 2007). UDP-glucuronosyltransferase, UGT1A1, plays a critical role in the detoxification of potentially neurotoxic bilirubin by conjugating it with glucuronic acid for excretion in bile (Ostrow and Murphy, 1970) and conjugates drugs and other xenobiotics (Radominska-Pandya et al., 1999; Tukey and Strassburg, 2000). Reduced bilirubin glucuronosyltransferase (UGT1A1) activity is associated with the development of unconjugated hyperbilirubinemia (Crigler-Najjar syndrome and Gilbert's syndrome) (Mackenzie et al., 1997) and increased side effects of drug treatment such as the predisposition of patients to toxicity initiated by SN-38, an active metabolite of the anticancer drug irinotecan (Gange et al., 2002; Tukey et al., 2002). Understanding the molecular mechanisms of the induction of human UGT1A1 may provide information for the prevention and treatment of unconjugated hyperbilirubinemia and the side effects of drugs. We identified a phenobarbital – responsive enhancer module at -3499/-3210 from the transcription start site of *UGT1A1*, gtPBREM (Sugatani et al., 2001). gtPBREM is a composite 290-bp element consisting of CAR-, PXR-, aryl hydrocarbon receptor (AhR)-, glucocorticoid receptor (GR)-, peroxisome proliferator-activated receptor α (PPARα)- and NF-E2-related factor 2 (Nrf2)-response elements (Sugatani et al., 2001; Sugatani et al., 2004; Yueh et al., 2003; Sugatani et al., 2005a; Senekeo-Effenberger et al., 2007; Yueh et al., 2007), and we demonstrated that the gtNR1 (-3382/-3367) within gtPBREM plays a central role in the expression of UGT1A1 mediated by both CAR and PXR (Sugatani et al., 2005b).

We previously demonstrated that (1) hepatocyte growth factor (HGF) increased mRNA and protein levels of UGT1A1 and CYP2B6 as well as the endogenous cyclin-dependent kinase (CDK)

DMD Fast Forward. Published on July 24, 2012 as DOI: 10.1124/dmd.112.046748
This article has not been copyedited and formatted. The final version may differ from this version.

2/4 inhibitors p16, p21, and p27 in HepG2 cells, (2) the CDK inhibitor roscovitine also enhanced the expression of UGT1A1, CYP2B6, and CYP3A4, and (3) transfection of anti-CDK2 siRNA led to elevated levels of UGT1A1, CYP2B6, and CYP3A4 in HepG2 cells (Sugatani et al., 2010). While HGF is a potent mitogen for hepatocytes, it is an antimitogenic factor for some tumor cell lines including HepG2; HGF induces p16 and p21 expression and decreases CDK2 activity, leading to inhibition of cell growth (Shima et al., 1998; Han et al., 2005). We furthermore found that CDK2 activity was decreased in HGF-treated HepG2 cells and there was a clear dissociation among the activation of CDK2 and the expression of UGT1A1, CYP2B6, and CYP3A4. T hus we concluded that the expression of UGT1A1 and CYP2B6 is negatively regulated through a CDK2 signaling pathway linked to cell cycle progression in HepG2 cells. Lin et al. (2008) demonstrated that roscovitine activates PXR-mediated *CYP3A4* gene expression through inhibition of CDKs in a ligand-independent manner, and that CDK2 negatively regulates the activity of PXR in HepG2 cells. However, it remains to be fully elucidated how the expression of UGT1A1 is r egulated through PXR or other nuclear receptors by roscovitine.

Thus, in this study, we investigated the nuclear receptor involved in the roscovitine-stimulated expression of UGT1A1 in HepG2 cells, and found that PXR contributes to the expression, using cells expressing CAR, PXR, and AhR. It remains to be clarified whether the regulatory mechanism of *UGT1A1* gene expression through PXR stimulation by roscovitine is different from that by rifampicin in a ligand-dependent manner. PXR activity has been shown to be modulated by translocation from the cytoplasm to nucleus, and the formation of heterodimers with retinoid X receptor (RXR) and interaction with co-factors in the nucleus (Squires et al., 2004; Timsit and Negishi, 2007). CAR and PXR form a complex with cytoplasmic CAR retention protein (CCRP; designated Dnajc7 in the NCBI data base) and heat shock protein (Hsp) 90 to maintain the cytoplasmic localization (Kobayashi et al., 2003; Squires et al., 2004). Phosphorylation of PXR at specific amino acid residues and other post-translational modifications modulate the cytoplasmic localization and the nuclear activation which affect the PXR activity

DMD Fast Forward. Published on July 24, 2012 as DOI: 10.1124/dmd.112.046748
This article has not been copyedited and formatted. The final version may differ from this version.

(Lichti-Kaiser et al., 2009a; Pondugula et al., 2009; Staudinger et al., 2011). We here identified critical residues involved in the enhanced expression of UGT1A1 by roscovitine compared with those by rifampicin, and investigated the role of the post-translational modification in PXR activation leading to the induction of UGT1A1 expression.

DMD Fast Forward. Published on July 24, 2012 as DOI: 10.1124/dmd.112.046748
This article has not been copyedited and formatted. The final version may differ from this version.

Materials and Methods

Materials. Roscovitine and MG-132 were purchased from Calbiochem (Darmstadt, Germany). Rifampicin and benzo[a]pyrene (B[a]P) were obtained from Sigma-Aldrich (St. Louis, MO). Actinomycin D was from P-L Biochemicals (Milwaukei, Wis, USA), adenosine-*S*-triphosphate (ATP) from Roche Diagnostics (Mannheim, Germany), and [γ-^{32}P]ATP from PerkinElmer (Santa Clara, CL, USA). All other chemicals and solvents were of analytical grade and obtained from commercial sources.

Plasmids. Reporter plasmids containing the UGT1A1 -3570/-3180 fragment linked to the -165/-1 fragment-pGL4-tk-firefly luciferase have been described (Sugatani et al., 2008). The expression vector pcDNA3.1-human steroid receptor coactivator (SRC)-2 has also been described (Sugatani et al., 2005a). The human CAR, human PXR, and human SRC-1 expression vectors were generously provided by Dr. Masahiko Negishi (National Institute of Environmental Health Sciences, NC, USA). The human AhR and human ARNT expression vectors were from Dr. Yoshiaki Fujii-Kuriyama (University of Tokyo, Tokyo, Japan). Mutations of PXR were performed with a QuickChange site-directed mutagenesis kit (Stratagene, La Jolla, CA, USA) according to the manufacturer's instructions (Sugatani et al., 2005a). The primers used were;
5'-CTATCACTTCAATGTCATGGCATGTGAAGGATGCAAGGG-3',
5'-CTGGCTATCACTTCAATGTCATGGATTGTGAAGGATGCAAGGGCTTTTT-3',
5'-CAGGGGTGCTTAGCGCTGGCTGCGAGTTGC-3',
5'-CCAGGGGTGCTTAGCGATGGCTGCGAGTTGCC-3',
5'-CTCTGCAGGCCCCAGCGAGGGAAGAAG-3',
5'-CAGAGTCTCTGCAGGCCCCAGATAGGGAAGAAGCTGCC-3',
5'-TCCGGAAAGATCTGTGCGCTTTGAAGGTCTCTCTG-3',
5'-GGTCCGGAAAGATCTGTGCGATTTGAAGGTCTCTCTGCAG-3',
5'-ACCCCCAGCCGACGCTGGCGGGAAAGAG-3',
5'-CAAACCCCCAGCCGACGATGGCGGGAAAGAGATC-3',

DMD Fast Forward. Published on July 24, 2012 as DOI: 10.1124/dmd.112.046748
This article has not been copyedited and formatted. The final version may differ from this version.

5'-CGAGGACCAGATCGCCCTGCTGAAGGG-3',

5'-ATCGAGGACCAGATCGACCTGCTGAAGGGGGC-3',

5'-GTCAACTGAGATTCAACGCAGTGTTCAACGCGGAG-3',

5'-CTGTGTCAACTGAGATTCAACGATGTGTTCAACGCGGAGACTGGA-3',

5'-GTGTGGCCGGCTGGCCTACTGCTTGGA-3',

5'-GGAGTGTGGCCGGCTGGACTACTGCTTGGAAGAC-3',

5'-CATCTCCCTCTTCGCCCCAGACCGCCC-3',

5'-CCATCTCCCTCTTCGACCCAGACCGCCCAG-3',

5'-CAATGCTCAGCACGCCCAGCGGCTGCT-3',

5'-ATCAATGCTCAGCACGACCAGCGGCTGCTGCG-3'

and their complements for human PXR T57A, T57D, S180A, S180D, S192A, S192D, S208A, S208D, S231A, S231D, S274A, S274D, T290A, T290D, S305A, S305D, S350A, S350D, T408A, and T408D, respectively. V ectors for the expression of 1) pCR3-human CAR-ΔC8, 2) pCR3-human PXR-ΔC9, 3) GST-human PXR and 4) YFP-human PXR were constructed by inserting the corresponding cDNAs, which were amplified by PCR with the primers; 1) 5'-gtttcc*ggatcc*ATGGCCAGTAGGGAAGATGAGCT-2' and 5'-gtttaa*ctcgag*TCACATCATGGCAGACAGG-3', 2) 5'-gtttcc*ggatcc*ATGGAGGTGAGACCCAAAGAAAGC-3' and 5'-gtttaa*ctcgag*TCACATGAGGGGCGTAGCAAAGGGGTG-3', 3) 5'-ttcaag*ggatcc*ATGGAGGTGAGACCCAAAGAA-3' and 5'-gtcttc*ctcgag*TCAGCTACCTGTGATGCCGAA-3', and 4) 5'-ttcaag*ctcgag*CTATGGAGGTGAGACCCAAAGAA-3' and 5'-gtcttc*ggatcc*TCAGCTACCTGTGATGCCGAA-3', respectively, into the *BamH* I and *Xho* I sites of pCR3 and pGEX-6P-3 (GE Healthcare Japan, Tokyo, Japan) and *Xho* I/ *BamH* I sites of pEYFP-C1 (Clontech Labolatories, CA) digested with the same enzymes, respectively. Bases in lower-case letters were added to allow digestion of the oligonucleotides with the restriction

enzymes. CAR-ΔC8 and PXR-ΔC9 were generated by the deletion of eight and nine amino acids from the C terminus, respectively. All e xpression vectors were sequenced by dye-terminator automated sequencing.

Cell Culture, Transfection, and Luciferase Assays. Human liver-derived cells (HepG2 cells line, RIKEN BioResource Center) and SW480 human colon cancer cells (American type culture collection) were seeded onto 24-well plates at 1 x 10^5 cells/ml in Dulbecco's modified Eagle medium (DMEM) and RPMI 1640 medium supplemented with 10% fetal calf serum (Hyclone), respectively. Twenty-four hours later, HepG2 cells were transfected with UGT1A1-luciferase reporter constructs including the distal (-3570/-3180) and proximal (-165/-1) regions (Sugatani et al., 2008) (0.2 μg) and expression vectors [pCR3-CAR (0.2 μg), pCR3-CAR (0.2 μg), pCR3-PXR (0.2 μg), or pCR3-AhR (0.2 μg) and pCR3-ARNT (0.2 μg), and pRL-SV40 (0.2 μg)] using a calcium phosphate co-precipitation method (CellPhect Transfection Kit, GE Healthcare Japan). The medium (1 ml per well) was replaced after 12 h with the same medium. The cells were subsequently treated for 24 h with roscovitine (1 x 10^{-7} to 1 x 10^{-5} M) or rifampicin (5 x 10^{-6} M) plus roscovitine (1 x 10^{-7} to 1 x 10^{-5} M) as 400 x concentrated stocks in dimethylsulfoxide; controls received an equivalent volume of dimethylsulfoxide. The total amount of DNA transfected was held constant in each transfection by using the corresponding empty vector. Transfected cells were washed once in phosphate-buffered saline and harvested in 1 x passive lysis buffer, and luciferase activity was measured simultaneously with the Dual-Luciferase reporter assay system according to the manufacturer's instructions (Promega, Madison, WI, USA); the firefly luciferase values were normalized to the *Renilla* values for each sample.

Quantitative Real-Time PCR. HepG2 cells (2 x 10^5) seeded onto 6-well plates and cultured for 24 h were transfected with expression vectors [pCR3 (0.2 μg), pCR3-CAR (0.2 μg), pCR3-CAR-ΔC8 (0.2 μg), pCR3-PXR (0.2 μg), pCR3-PXR-ΔC9 (0.2 μg), or pCR3-PXR mutant (0.2 μg)] or [pCR3 (0.2 μg), pCR3-PXR (0.2 μg), or pCR3-PXR mutant (0.2 μg) and pcDNA3.1 (0.2 μg),

pcDNA3.1-SRC-1 (0.2 μg), or pcDNA3.1-SRC-2 (0.2 μg)] using TransIT-LT1 (Mirus Bio, Madison, WI) according to the manufacturer's instructions. At 24 h after transfection, cells were given fresh medium and further transfected with the expression vectors, and then cultured with roscovitine (5 μM) or vehicle for an additional 24 h unless otherwise stated; the transfection efficiency was increased by the repeat transfection compared to the single transfection [the level of PXR mRNA was increased 2.29 $\pm$ 0.02 fold and the levels of UGT1A1 mRNA induced by roscovitine and rifampicin were increased 2.96 $\pm$ 0.15 and 3.44 $\pm$ 0.14 fold by the repeat transfection with pCR3-PXR expression vector, respectively (n=4)]. Total RNA was extracted using TRIZOL reagent from Invitrogen, and cDNAs were synthesized with a PrimeScript RT reagent kit (TaKaRa Bio, Otsu, Japan) according to the directions. cDNA synthesized from 100 ng of total RNA was subjected to quantitative real-time PCR with an ABI PRISM 7000 Sequence Detector (Applied Biosystems, Foster City, CA) using Premix Ex Taq reagent (TaKaRa Bio Inc., Otsu, Japan) for the TaqMan probe method or SYBR Premix Ex Taq reagent (TaKaRa Bio Inc.) for the intercalation reaction with SYBR Green I according to the manufacturer's specifications for UGT1A1 (NM_000463) and CYP3A4 (NM_017460) as described previously (Sugatani et al., 2010) and CDK5 (NM_004935; HA077276, TaKaRa Bio Inc), by using Assays-on Demand Gene Expression Products for CDK1 (NM_001786; Hs00936776_m1) and CDK2 (NM_001798; Hs01548894_m1) (Applied Biosystem), or by using Pre-Developed Taq Man Assay Reagent for β-actin (NM_001101) (Applied Biosystem). The thermal cycle conditions were as follows: hold for 10 sec at 95^{o}C, followed by two-step PCR for 40 cycles of 95^{o}C for 5 sec followed by 60^{o}C for 30 sec. β-Actin was used to normalize gene expression in all samples. Fold-induction values were calculated by subtracting the mean difference of gene and β-actin cycle threshold Ct numbers for each treatment group from the mean difference of gene and β-actin Ct numbers for the vehicle group and raising the difference to the power of 2 ($2^{-\Delta\Delta Ct}$).

Western Blot Analysis. HepG2 cells (2×10^6) seeded into 75 cm^2 flasks and cultured for 24 h

were transfected with expression vectors [pCR3 (10 μg), pCR3-CAR (10 μg), pCR3-PXR (10 μg), pEYFP (10 μg), pEYFP-PXR (10 μg), or pEYFP-PXR mutant (10 μg)] using TransIT-LT1 (Mirus Bio, Madison, WI) according to the manufacturer's instructions. At 24 h after transfection, cells were given fresh medium and further transfected with the expression vectors, and then cultured with roscovitine (5 μM) or vehicle for an additional 24 h unless stated otherwise. Treated and untreated cells were washed three times with ice-cold phosphate-buffered saline and lysed with a freshly prepared lysis buffer containing 50 mM Tris-HCl (pH 7.4), 1% NP-40, 0.25% sodium deoxycholate, 150 mM NaCl, 1 mM EDTA, 1mM phenylmethylsulfonyl fluoride, 1 mM Na_3VO_4, 1 mM NaF, 1 mM benzamidine, 1 μg/ml aprotinin, and 1 μg/ml leupeptin at 4°C. The lysates were centrifuged at 110,000 g for 10 min. Nuclear extracts and cytoplasmic fractions were prepared using a nuclear extract kit (Active Motif). The cytoplasmic fractions including microsomal proteins were used to investigate the expression of UGT1A1 and CYP3A4. The protein concentrations were determined by the Bradford assay (Bio-Rad). Western blotting was performed as described (Osabe et al., 2008). Briefly, nuclear extracts, cytoplasmic fractions, or cell lysates (50 μg) were resolved on 12.5% SDS-polyacrylamide gels and the proteins were transferred electrophoretically to polyvinylidene difluoride membranes (Milipore Corporation, Bedford, MA). Membranes were blocked at 4°C overnight in Blocking One (Nacalai Tesque, Kyoto, Japan) and probed for 1 h with primary antibodies including anti-UGT1A1 and anti-CYP3A4 from BD Gentest (Woburn, MA), anti-PXR (sc-7737), anti-RXR (sc-553), and anti-Histone H1 (sc-8030) from Santa Cruz Biotechnology (Santa Cruz, CA), anti-HSP90 (#4874), anti-acettylated lysine (#9814), and anti-histoe deacetylases 1, 2, 3, 4, 5, and 7 (#9928) from Cell Signaling Technology (Danvers, MA), anti-green fluorescent protein from Medical Biological Laboratories (Nagoya, Japan), anti-CCRP from Abnova (Taipei, Taiwan), and anti-α-tubulin from Oncogene Research Products (Boston, MA). Antigen-antibody complexes were detected using the appropriate secondary antibody conjugated to horseradish peroxidase [horseradish peroxidase-conjugated anti-rabbit, anti-goat, or anti-mouse

immunoglobulin (Jackson Immuno Research)] and visualized with an enhanced chemiluminescence system (GE Healthcare UK Ltd., Little Chalfont, England).

Small Interfering RNA-Mediated Protein Knockdown. s iRNAs targeting human CDK1 (stealth RNAi HSS190656), human CDK2 (validated stealth RNAi VHS40359), and human CDK5 (stealth RNAi HSS101730) were obtained from Invitrogen Life Technology (Carlsbad, CA, USA). SW480 cells cultured for 24h were transfected with siRNA duplexes (100 nM) using TransIT-siQUEST (Mirus Bio, Madison, WI) according to the manufacturer's instructions. At 24 h after transfection, cells were given fresh medium and further transfected with the siRNA duplexes for an additional 24 h unless stated otherwise.

In Vitro Kinase Assay. GST-PXR and GST-PXR S350D fusion proteins were expressed in *Escherichia coli* BL21 [DE3(pLys)] and purified using glutathione-Sepharose (Amersham Biosciences) according to the manufacturer's protocols. CDK2 kinase assays were performed as described previously (Sugatani et al., 2010). Cell lysates prepared from SW480 cells at 2 h after release from the thymidine block (Osabe et al., 2008) were cleared by centrifugation, and equal amounts of protein in the cell extracts (50 μg) were immunoprecipitated with 1 μg of anti-CDK2 antibody for 3 h at 4^{o}C. Precipitated immune complexes were washed three times with the cell lysis buffer and twice with a kinase buffer [50 mM Tris-HCl, (pH 7.5) containing 10 mM $MgCl_2$, 1 mM dithiothreitol, 20 mM EGTA, 10 mM β-glycerophoshate, 0.1 mM sodium orthovanadate, and 1 mM NaF]. Kinase reactions were performed in 10 μl of the kinase buffer containing 25 μg of GST-fused protein, 100 μM ATP, and 0.37 MBq of [γ-^{32}P]ATP at 30^{o}C for 30 min. Reactions were stopped by addition of 10 μl of 2 x Laemmli sample buffer (125 mM Tris-HCl (pH 6.8), 4% SDS, 20% glycerol, 0.002% bromophenol blue, and 10% 2-mecaptoethanol) and samples were resolved by SDS-PAGE on a 5 to 20% gradient gel (ATTO Corporation, Tokyo, Japan) after heat denaturation. Phosphorylation of the substrate was visualized by autoradiography.

Immunocytochemistry. To detect the localization of PXR and PXR mutants, HepG2 cells (6 x

10^3 /well) seeded on 3-well glass coverslips (Teflon printed glass slides, Eric Scientific Company) were transfected with expression vectors [pEYFP (0.2 μg), pEYFP-PXR (0.2 μg), or pEYFP-PXR mutant (0.2 μg)] using TransIT-LT1 (Mirus Bio, Madison, WI) according to the manufacturer's instructions. At 24 h after transfection, cells were given fresh medium and further transfected with the expression vectors, then cultured with roscovitine (5 μM) or vehicle for an additional 24 h. Cells were fixed with methanol and nuclein was stained with 3 μM 4,6-diamidino-2-phenylindole-2-HC (DAPI, Dojindo Laboratories, Kumamoto, Japan). Subsequently, cells were washed and mounted with Antifade reagent (Bio-Rad). Fluorescence was visualized using a LSM510 confocal microscope (Carl Zeiss AG). For quantitation, the subcellular localization of YFP-PXR, YFP-PXR T290D, YFP-PXR S350D, and YFP-PXR T408D was scored in at least 100 cells.

Coimmunoprecipitation. HepG2 cells (2 x 10^6) seeded into 75 cm^2 flasks and cultured for 24 h were transfected with expression vectors [pEYFP (10 μg), pEYFP-PXR (10 μg), or pEYFP-PXR mutant (10 μg)] using TransIT-LT1 (Mirus Bio, Madison, WI) according to the manufacturer's instructions. At 24 h after transfection, cells were given fresh medium and further transfected with the expression vectors, and cultured with roscovitine (5 μM) or vehicle for an additional 24 h. The nuclear extract (280 μg) or cytoplasmic fraction (460 μg) was pre-cleared with protein G agarose beads and rabbit IgG (Santa Cruz Biotechnology, Santa Cruz, CA) for 30 min at 4^{o}C. YF P-tagged proteins were immunoprecipitated using the anti-GFP antibody or anti-CCRP antibody combined with the protein G agarose beads. The agarose beads were washed three times with Dulbecco's phosphate buffer and subjected to SDS-PAGE on a 5 to 20% gradient gel (ATTO Corporation, Tokyo, Japan). The proteins were transferred to an immobilon-P transfer membrane (Millipore), and the blots were probed with antibodies as indicated.

Statistics. Values are expressed as the mean ± standard error. All data were analyzed using a one-way analysis of variance. T he statistical significance of differences between groups was

analyzed using the ANOVA or an unpaired *t*-test. The level for statistically significant differences was set at $p<0.05$.

Results

Enhancement of PXR-mediated transactivation of *UGT1A1* gene by the CDK inhibitor roscovitine. Previously (Sugatani et al., 2010), we found that roscovitine stimulated markedly the expression of UGT1A1 mRNA and protein, but only slightly that of CYP1A1, CYP2B6, and CYP3A4 mRNA and protein, in HepG2 and SW480 cells. To investigate the transactivation mechanism for UGT1A1 expression induced by roscovitine, we investigated the transcriptional activities of a distal (-3570/-3180) enhancer motif linked to a proximal (-165/-1) promoter motif placed in front of the reporter luciferase gene in HepG2 cells in the presence of exogenously expressed CAR, PXR, or AhR/ aryl hydrocarbon nuclear translocator (ARNT). PXR-mediated transactivation of the reporter gene in the absence of rifampicin was enhanced by roscovitine in a dose-dependent manner and peaked at 5 μM roscovitine (Fig. 1). The extent of PXR-mediated transactivation by 5 μM roscovitine was almost the same as that by 5 μM rifampicin. The PXR-mediated transcriptional activity of the reporter gene in the absence of rifampicin with 5 μM roscovitine (3.3 ± 0.1-fold the control) was more prominently enhanced, compared with the basal activity (1.9 ± 0.1 fold the control), CAR-mediated activity (1.4 ± 0.1-fold the control), PXR-mediated activity in the presence of 5 μM rifampicin (1.1 ± 0.0-fold the control), and AhR/ARNT-mediated activity in the absence and presence of benzo[a]pyrene (1.1 ± 0.0- and 1.4 ± 0.0-fold the control, respectively) (Fig. 1).

Moreover, to evaluate the role of PXR in the induction of UGT1A1 expression by roscovitine, the basal, CAR- or PXR-expressing plasmid was transfected into HepG2 cells. The mRNA level of UGT1A1 in the cells expressing exogenous PXR was markedly enhanced by roscovitine (52.2 ± 7.2-fold), compared with levels in the control cells and the cells expressing CAR (8.7 ± 1.8- and 2.7 ± 0.2-fold, respectively), and that of CYP3A4 in the cells expressing PXR was also enhanced by roscovitine (3.6 ± 0.6-fold) but not in the cells expressing CAR (Fig. 2A and 2B). The induction of UGT1A1 and CYP3A4 mRNA expression by PXR stimulated by roscovitine was abolished by

DMD Fast Forward. Published on July 24, 2012 as DOI: 10.1124/dmd.112.046748
This article has not been copyedited and formatted. The final version may differ from this version.

the deletion of eight and nine amino acids from the C-terminus of CAR (CAR -ΔC8) and PXR (PXR-ΔC9), respectively. Furthermore, the protein levels of UGT1A1 and CYP3A4 were enhanced by roscovitine in the cells that expressed PXR. The levels of UGT1A1 and CYP3A4 were also enhanced in the cells expressing CAR, but slightly and not by roscovitine, respectively (Fig. 2C).

Effects of phosphomimetic and phosphodeficient mutations of PXR on *UGT1A1* expression stimulated by roscovitine and rifampicin. To determine whether the regulatory mechanism of *UGT1A1* expression through PXR stimulation by roscovitine is different from that by the PXR ligand rifampicin, we were prompted to investigate effects of phosphomimetic mutations of PXR on *UGT1A1* and *CYP3A4* expression stimulated by roscovitine and rifampicin. T57, S180, S192, S208, S230, S274, T290, S305, S350 and T408 were selected for mutagenesis, based on "in silico" consensus kinase site predictions and the reports by Lichti-Kiser et al. (2009a) and Pondugula et al. (2009). As shown in Figures 3 and 4, phosphomimetic mutations at T57, T290, S350, and T408 attenuated the induction of UGT1A1 and CYP3A4 mRNA expression by roscovitine. Although it was not easy to determine the residues associated with the induction of CYP3A4 mRNA by roscovitine and rifampicin, it resulted from UGT1A1 mRNA being more stable than CYP3A4 mRNA (Fig. 5). Accordingly, we determined the residues associated with PXR transactivation capacity for *UGT1A1* expression by roscovitine and rifampicin. Phosphomimetic mutations at T57, S274, T290, S305, S350, and T408 reduced the induction of UGT1A1 mRNA expression by rifampicin to below 0.5-fold that by the wild-type PXR (Figs. 3 and 4). Both the phosphmimetic mutation and the phosphodeficient mutation at T57 attenuated PXR activation by rifampicin and roscovitine (Fig. 4). The S350D mutation attenuated the activation by roscovitine, whereas the phosphodeficient mutation increased it (Fig. 4).

S350 is involved in the down-regulation of UGT1A1 expression and phosphorylation of PXR by CDK2. In a previous study (Sugatani et al., 2010), transfection with the anti-CDK2 siRNA in HepG2 and SW480 cells led to stimulated expression of UGT1A1, CYP2B6, and CYP3A4 mRNAs

and proteins, with the extent of the stimulation by anti-CDK2 siRNA greater in SW480 cells than in HepG2 cells. Since roscovitine is a CDK1, CDK2, and CDK5 inhibitor (Meijer et al., 1997), anti-CDK1 siRNA, anti-CDK2 siRNA, or anti-CDK5 siRNA was introduced into SW480 cells. Transfection with the anti-CDK2 siRNA was followed by an increase in the UGT1A1 mRNA level, but transfections with anti-CDK1 siRNA and anti-CDK5 siRNA were not (Fig. 6A). Since the residue at S350 is predicted to be the only one phosphorylated by cyclin-dependent kinase in the PXR protein, we analyzed the extent of phosphorylation of a GST-PXR or GST-S350D PXR fusion protein after incubation with the cell lysate. As shown in Fig. 6B, the extent of phosphorylation was decreased in S350D-mutated PXR compared with wild-type PXR and CDK2 activity was required for down-regulation of UGT1A1 expression by roscovitine.

Effects of phosphomimetic mutations at T290, S350, and T408 on the subcellular localization of the PXR proteins. We next investigated whether a phosphomimetic mutation alters the nuclear translocation of PXR in HepG2 cells treated with roscovitine and contributes to impaired transcriptional activity. The S350D mutant YFP-PXR fusion protein was decreased in the cytoplasm and accumulated in the nucleus after roscovitine treatment, similar to the wild-type protein (Fig. 7). The T290D and T408D mutant YFP-PXR fusion proteins were retained in the cytoplasm and the translocation of both mutant proteins to the nucleus by roscovitine was suppressed (Fig. 7A). The level of the T290D and T408D mutants in the cytoplasm was higher than that of the wild-type protein, whereas the expression of the T408D mutant was lower than that of the T290D mutant (Fig. 7B). However, the levels of the T408D mutant in the cytoplasm were markedly elevated after treatment with proteasome inhibitor MG-132, in the presence and absence of roscovitine, compared with those of the wild-type protein (Fig. 7C). Immunocytochemistry revealed that the S350D mutant YFP-PXR protein but not T290D and T408D mutant proteins was localized to the nucleus in the cells stimulated by roscovitine similar to the wild-type protein (Fig. 8). In contrast, the T290D and T408D mutant YFP-PXR proteins revealed a punctate distribution in the cytoplasm and nucleus of the cells treated with and without roscovitine. These observations

DMD Fast Forward. Published on July 24, 2012 as DOI: 10.1124/dmd.112.046748
This article has not been copyedited and formatted. The final version may differ from this version.

indicate that phosphorylation at T290 and T408 abrogated the roscovitine-stimulated nuclear translocation capacity of PXR and resulted in its impaired function.

SRC-2 partly recovers the impaired transcriptional activity of S350D mutant PXR in HepG2 cells. Since transcriptional co-activators promote the function of nuclear receptors (Glass et al., 2000), we investigated effects of SRC-1 and SRC-2 on impaired transcriptional activity of S350D mutant PXR in HepG2 cells. Whereas SRC-1 and SRC-2 did not alter the transcriptional activities of the basal and exogenously expressed wild-type PXR by roscovitine, SRC-2 but not SRC-1 enhanced the impaired activity of the S350D mutant 1.5-fold, indicating that phosphorylation at S350 is likely to alter the binding affinity of PXR with a coactivator such as SRC-2 (Fig. 9).

Role of HSP90 and CCRP in cytoplasmic localization of T290D and T408D mutant YFP-PXR fusion proteins. HSP90 and CCRP are involved in maintaining the cytoplasmic localization of PXR (Squires et al., 2004). To test whether HSP90 or CCRP was involved in the retention of the T290D and T408D mutant YFP-PXR proteins in the cytoplasm, we investigated whether the mutants formed a complex with HSP90 or CCRP in the cytoplasm. Immunoprecipitation with anti-GFP or anti-CCRP antibody and western blot analyses demonstrated that the wild-type and T290D and S350D mutant PXR proteins (Fig. 10A) but not YFP protein (data not shown) in the cytoplasm formed a complex with HSP90 and CCRP. The formation of a T290D mutant PXR - HSP90 - CCRP complex was not disrupted even after roscovitine treatment. In contrast, little T408D mutant - HSP90 - CCRP complex was found in the cells treated with or without roscovitine (Fig. 10A), suggesting that HSP and CCRP contribute to the retention of the T290D but not T408D mutant in the cytoplasm.

Phosphomimetic mutation at S350 alters deacetylation of PXR and capacity to bind with RXR in the nucleus of cells treated with roscovitine. Next, we investigated the effect of a phosphomimetic mutation at S350 on PXR activation in the nucleus by roscovitine, that is, heterodimerization with RXR and release from acetylation after roscovitine treatment. PXR forms a heterodimer with RXR and helps to activate PXR. Whereas the YFP protein was markedly

expressed compared with the YFP-PXR fusion protein and an association of YFP with RXR was found, the extent of binding of the wild-type YFP-PXR fusion protein with RXR was more than that of YFP with RXR and further enhanced by roscovitine, but that of the S350D mutant with RXR was markedly reduced (Fig. 10B). Since the levels of the wild-type and S350D mutant PXR proteins were lower in the nucleus of the control cells than that of the roscovitine-treated cells, acetylated forms were detected in trace amounts (Fig. 10B). However, western blot analysis utilizing anti-acetyl-lysine (ACK) antibody demonstrated that acetylated S350D mutant YFP-PXR protein but not the wild-type or YFP protein was detected even in the nucleus after roscovitine treatment, although the levels of the wild-type and S350D mutant proteins were similar (Fig. 10B). Furthermore, whereas the level of binding of wild-type YFP-PXR fusion protein with histone deacetylase (HDAC) 1 was enhanced after roscovitine treatment, that of the S350D mutant with HDAC1 was reduced (Fig. 10B). In addition, the level of binding of the S350D mutant PXR with HDAC3 was also reduced after roscovitine treatment, compared with the wild-type protein (Fig. 10B). These results suggest that the wild-type YFP-PXR fusion protein but not S350D-mutated protein may be deacetylated by HDAC after roscovitine stimulation.

Discussion

PXR, a member of the nuclear orphan receptor superfamily, was originally characterized as a xenobiotic-activated transcription factor that plays a key role in regulating the activation of genes encoding drug-metabolizing enzymes and drug transporters and subsequently has been found to potentiate a variety of biological effects associated with pharmacological and toxicological consequences (reviewed in Timsit and Negishi, 2007; Staudinger and Lichti, 2008; Ihunnah et al., 2011) and hepatic energy metabolism including gluconeogenesis, β-oxidation of fatty acids, and lipogenesis (reviewed in Konno et al., 2008). Upon the binding of endogenous and exogenous xenobiotics to its ligand-binding domain (LBD), PXR is activated and translocated from the cytoplasm to cell nucleus where it allows interaction with coactivators such as SRC-1 and SRC-2 and activates transcription by binding to the xenobiotic-response element in the promoter region of the target gene. Recent studies demonstrated that post-translational modifications of PXR alter its function; Lin et al. (2008) showed that CDK2 directly phosphorylates PXR and negatively affects its activity, and Biswas et al. (2011) found that the acetylation status of PXR regulates its selective function independent of ligand activation. Thus, while post-translational modifications of PXR are likely to be involved in the regulation of its function, much less is known about the molecular mechanism regulating physiological functions of PXR. Our finding that the CDK inhibitor roscovitine markedly stimulated the expression of UGT1A1 mRNA and protein in HepG2 cells (Sugatani et al., 2010) prompted us to investigate how roscovitine enhances *UGT1A1* gene expression. In the reporter gene assay, PXR-mediated transcriptional activity of the reporter gene was more prominently enhanced by roscovitine, compared with the basal, CAR-mediated, and AhR/ARNT-mediated transcriptional activities (Fig. 1). Moreover, expression of UGT1A1 mRNA and protein was markedly enhanced by roscovitine in HepG2 cells expressing PXR (Fig. 2). These observations indicate that PXR contributes to the induction of UGT1A1 expression by roscovitine.

Since roscovitine has been shown to activate PXR with moderate effect but bind to PXR with

DMD Fast Forward. Published on July 24, 2012 as DOI: 10.1124/dmd.112.046748
This article has not been copyedited and formatted. The final version may differ from this version.

lower affinity than the PXR ligand SR12813 (Lin et al., 2008), in the present study, we investigated the mechanism of PXR activation to induce UGT1A1 expression both in a ligand-independent manner by roscovitine and in a PXR ligand rifampicin-inducible manner. We analyzed roles of 9 potential phosphorylation sites in the ligand-binding domain (LBD) demonstrated using in silico consensus site prediction methods and reporter gene analysis by Lichti-Kaiser et al. (2009a), compared with the functionally significant T57 site in the DNA-binding domain (DBD) (Pondugula et al., 2009). Phosphomimetic mutations at T290, S350, and T408 of PXR strongly attenuated the induction of UGT1A1 expression by roscovitine as did the phosphomimetic mutation at T57, while those at T290, S305, and T408 contributed to the suppression of rifampicin-stimulated UGT1A1 expression (Figs. 3 and 4). As expected, some of the residues involved in PXR activation by roscovitine and rifampicin are different. In both rifampicin- and roscovitine-stimulated cells, the T57 phosphomimetic mutant PXR lost all transcriptional activity for the *UGT1A1* gene (Figs. 3 and 4). Pondugula et al. (2009) found that T57 identified as a potential phosphorylation site for p70 S6K is located in the first zinc-finger motif of the DBD and the mutation T57D impairs the ability to bind to the target CYP3A4 promoter. Thus, T57 is considered to play a key role in both ligand-inducible and ligand-independent PXR activation. In contrast, the phosphomimetic mutation at S305 more strongly reduced the ligand (rifampicin)-inducible transcriptional activity compared with the ligand-independent activation by roscovitine (Figs. 3 and 4), indicating that the residue at S305 in the LBD plays an important role in the ligand-dependent PXR activation. As reported by Lichti-Kaiser et al. (2009a), the impaired activity of the S305D mutant PXR may result from the inhibition of ligand-inducible PXR-RXR heterodimerization and interaction with its cofactors. On the other hand, in our previous study, we demonstrated that the expression of UGT1A1 is negatively regulated through a CDK2 signaling pathway linked to cell cycle progression in HepG2 cells, but the molecular mechanism remains to be clarified (Sugatani et al., 2010). Phosphomimetic mutation of the residue at S350 in only one consensus CDK phosphorylation motif [(S/T)PX(R/K)] more strongly impaired the roscovitine-stimulated

transcriptional activity compared with the ligand-inducible activity, whereas the interaction of the S350D mutant PXR with RXR after roscovitine treatment was markedly reduced in coimmunoprecipitation assays (Figs. 3, 4, and 10). In addition, SRC-2 but not SRC-1 enhanced the roscovitine-stimulated activity of the S350D mutant PXR (Fig. 9), although SRC-1 binding has been found to promote the specific interaction between ligands and PXR (Watkins et al., 2003). These observations indicate that phosphorylation at S350 is likely to alter the interaction of PXR with its coactivator and influence the formation of a complex with RXR and its coactivator, repressing the cell-based nuclear transactivation of PXR by roscovitine. This study demonstrated that the deletion of CDK2 but not CDK1 or CDK5 using siRNA resulted in enhanced UGT1A1 expression (Fig. 6A) and the wild-type PXR protein but not S350D mutant was phosphorylated by CDK2 (Fig. 6B). These findings that CDK2 phosphorylates the S350 residue of the PXR protein, resulting in impaired PXR activity, confirm the speculation by Lin et al. (2009) made based on a reporter gene analysis with mutant PXR protein. Moreover, the present study demonstrated that the S350D mutant but not wild-type PXR was detected as acetylated in the cell nucleus after roscovitine treatment (Fig. 10B). In addition, the level of binding of wild-type PXR with HDAC1 was increased in the cell nucleus after roscovitine treatment, but that of the S350D mutant was decreased (Fig. 10B). These results suggest that the PXR protein would be acetylated in the nucleus of the control cells, resulting in impaired PXR activity, and the deacetylation by HDAC may lead to the PXR activation. Recently, it has been shown that PXR is acetylated *in vivo* and the acetylation status of the PXR protein regulates its selective function independent of ligand activation (Biswas et al., 2011), and that HDAC1 is required for carbamazepine-induced CYP3A4 expression (Wu et al., 2012). While further study of whether HDAC1 is involved in PXR activation by roscovitine as well as by carbamazepine is required, an acetylated S350D mutant PXR may result in impaired activity in the nucleus.

Although site-specific phosphorylation has been shown to occur in the PXR protein to modulate its activity (Lin et al., 2008; Lichti-Kaiser et al., 2009a; Pondugula et al., 2009), the

current study has for the first time found the critical role of T290 in PXR activation. Phosphomimetic mutation at T290 of PXR also suppressed roscovitine-induced translocalization of the YFP-PXR fusion protein from the cytoplasm to nucleus, which may result in the reduced transcriptional activity of PXR in the cells stimulated by roscovitine and rifampicin (Figs. 3, 4, 7 and 8). The formation of a complex of PXR with HSP90 and CCRP has been found to retain PXR in the cytoplasm (Squires et al., 2004). Western blot and immunoprecipitation analyses demonstrated the presence of T290D mutant YFP-PXR in a complex with HSP90 and CCRP, and the extent of accumulation in the cytoplasm was not changed after roscovitine treatment (Figs. 7 and 10). While the ligand-independent mechanism regulating PXR activation remains to be clarified, the present finding demonstrated that phosphorylation at T290 is likely to suppress the roscovitine-induced dissociation of PXR from HSP90 and CCRP, resulting in the accumulation of PXR protein in the cytoplasm. The complex of T408D mutant PXR with HSP90 and CCRP was rare, but the T408D mutant protein was accumulated in the cytoplasm of the cells treated with MG-132. These observations indicate that PXR phosphorylated at T408 may be degraded by proteasome (Figs. 7 and 10), because murine PXR has been reported to be a target of proteasomal degradation (Masuyama et al., 2002). Protein kinase A (PKA) and protein kinase C (PKC) contribute to cell signaling involved in ligand-inducible PXR activation (Ding and Staudinger, 2005; Lichti-Kaiser et al., 2009b). PKC-dependent signaling has been demonstrated to repress the transcriptional activity of PXR by increasing the strength of interaction between PXR and the nuclear receptor co-repressor protein (Ding and Staudinger, 2005). Lichti-Kaiser et al. (2009b) demonstrated (1) that PKA signaling has a repressive effect upon PXR-mediated gene activation in human hepatocytes and stimulates the interaction of PXR with the nuclear receptor co-repressor, and (2) that human PXR protein can serve as an effective substrate for catalytically active PKA *in vivo*. Further study is needed to determine whether PKA or PKC associated with cell signaling contributes to the phosphorylation of PXR at T290 (a predicted PKA/PKC phosphorylation site).

In conclusion, whereas phosphorylation of PXR at T290 and T408 suppresses the PXR

activation both in a ligand-dependent manner by rifampicin and in a ligand-independent manner by roscovitine, roscovitine inhibits phosphorylation of PXR at S350 by CDK2 and enhances the translocation of PXR from the cytoplasm to the nucleus, resulting in elevated expression of UGT1A1. The current study provides a clue to examining dynamic regulatory mechanisms through post-translational modifications such as phosphorylation and acetylation and specific cross-talk with diverse signaling pathways in PXR activation.

Acknowledgments

We gratefully acknowledge Yoshinori Hattori for excellent technical assistance.

Authorship Contributions

Participated in research design: Sugatani

Conducted experiments: Sugatani, Uchida, Kurosawa

Contributed new reagents or analytic tools: Sugatani, Uchida, Kurosawa

Performed data analysis: Sugatani, Uchida, Kurosawa, Yamaguchi, Yamazaki, Ikari, Miwa

Wrote or contributed to the writing of the manuscript: Sugatani, Miwa

References

Biswas A, Pasquel D, Tyagi RK, Mani S (2011) Acetylation of pregnene X receptor protein determines selective function independent of ligand activation. *Biochem Biophys Res Commun* **406**: 371-376.

Ding X, Staudinger JL (2005) Repression of PXR-mediated induction of hepatic *CYP3A* gene expression by protein kinase C. *Biochem Pharmacol* **69**: 867-873.

Gagne JF, Montminy V, Belanger P, Journault K, Gaucher G, Guillemette C (2002) Common human UGT1A polymorphisms and the altered metabolism of irinotecan active metabolite 7-ethyl-10-hydroxycamptothecin (SN-38). *Mol Pharmacol* **62**: 608-617.

Glass CK, Rosenfeld MG (2000) The coregulator exchange in transcriptional functions of nuclear receptors. *Genes Dev* **14**: 121-141.

Han J, Tsukada Y, Hara E, Kitamura N, Tanaka T (2005) Hepatocyte growth factor induces redistribution of $p21^{CIP1}$ and $p27^{KIP1}$ through ERK-dependent $p16^{INK4a}$ up-regulation, leading to cell cycle arrest at G1 in HepG2 hepatoma cells. *J Biol Chem* **280**: 31548-31556.

Ihunnah CA, Jiang M, Xie W (2011) Nuclear receptor PXR, transcriptional circuits and metabolic relevance. *Biochim Biophys Acta* **1812**: 956-963.

Kobayashi K, Sueyoshi T, Inoue K, Moore R, Negishi M (2003) Cytoplasmic accumulation of the nuclear receptor CAR by a tetratricopeptide repeat protein in HepG2 cells. *Mol Pharmacol* **64**: 1069-1075.

Konno Y, Negishi M, Kodama S (2008) The roles of nuclear receptors CAR and PXR in hepatic energy metabolism. *Drug Metab Pharmacokinet* **23**: 8-13.

Lichti-Kaiser K, Brobst D, Xu C, Staudinger JL (2009a) A systematic analysis of predicted phosphorylation sites within the human pregnane X receptor protein. *J Pharmacol Exp Ther* **331**: 65-76.

Lichti-Kaiser K, Xu C, Staudinger JL (2009b) Cyclc AMP-dependent protein kinase signaling modulates pregnane x receptor activity in a species-specific manner. *J Biol Chem* **284**:

6639-6649.

Lin W, Wu J, Dong H, Bouck D, Zeng F-Y, Chen T (2008) Cyclin-dependent kinase 2 negatively regulates human pregnane X receptor-mediated *CYP3A4* gene expression in HepG2 liver carcinoma cells. *J Biol Chem* **283**: 30650-30657.

Mackenzie PI, Owens IS, Burchell B, Bock KW, Bairoch A, Belanger A, Fournel-Gigleux S, Green M, Hum DW, Iyanagi T, Lancet D, Louisot P, Magdalou J, Chowdhury JR, Ritter JK, Schachter H, Tephly TR, Tipton KF, Nebert DW (1997) The UDP glycosyltransferase gene superfamily: recommended nomenclature update based on evolutionary divergence. *Pharmacogenetics* **7**: 255-269.

Masuyama H, Inoshita H, Hiramatsu Y, Kudo T (2002) Ligands have various potential effects on the degradation of pregnane X receptor by proteasome. *Endoccrinology* **143**: 55-61.

Meijer L, Borgne A, Mulner O, Chong JPJ, Blow JJ, Inagaki N, Inagaki N, Delcros JG, Moulinoux JP (1997) Biochemical and cellular effects of rescovitine, a potent and selective inhibitor of the cyclin-dependent kinases cdc2, cdk2 and cdk5. *Eur J Biochem* **243**: 527-536.

Osabe M, Sugatani J, Takemura A, Yamazaki Y, Ikari A, Kitamura N, Negishi M, Miwa M (2008) Expression of CAR in SW480 and HepG2 cells during G1 is associated with cell proliferation. *Biochem Biophys Res Commun* **369**: 1027-1033.

Ostrow JD, Murphy NH (1970) Isolation and properties of conjugated bilirubin from bile. *Biochem. J.* **120**: 311-327.

Pondugula SR, Brimer-Cline C, Wu J, Schuetz EG, Tyagi RK, Chen T (2009) A phosphomimetic mutation at threonine-57 abolishes transactivation activity and alters nuclear localization pattern of human pregnane X receptor. *Drug Metab Dispos* **37**: 719-730.

Radominska-Pandya A, Czemik PJ, Little JM, BattagliaE, Mackenzie PI (1999) Structural and functional studies of UDP-glucuronosyltransferases. *Drug Metab Rev* **31**: 817-899.

Senekeo-Effenberger K, Chen S, Brace-Sinnokrak E, Bonzo JA, Yueh M-F, Argikar U, Kaeding J, Trottier J, Remmel RP, Ritter JK, Barbier O, Tukey RH (2007) Expression of the human *UGT1*

locus in transgenic mice by 4-chloro-6-(2,3-xylidino)-2-pyrimidinylthioacetic acid (WY-14643) and implications on drug metabolism through peroxisome proliferator-activated receptor a activation. *Drug Metab Dispos* **35**: 419-427.

Shima N, Stolz DB, Miyazaki M, Gohda E, Higashino K, Michalopoulos GK (1998) Possible involvement of p21/waf1 in the growth inhibition of HepG2 cells induced by hepatocyte growth factor. *J Cell Physiol* **177**: 130-136.

Squires EJ, Sueyoshi T, Negishi M (2004) Cytoplasmic localization of pregnane X receptor and ligand-dependent nuclear translocation in mouse liver. *J Biol Chem* **279**: 49307-49314.

Staudinger JL, Lichti K (2008) Cell signaling and nuclear receptors: New opportunities for molecular pharmaceuticals in liver disease. *Mol Pharm* **5**: 17-34.

Staudinger JL, Xu C, Biswas A, Mani S (2011) Post-translational modification of pregnane x receptor. *Pharmacol Res* **64**: 4-10.

Sugatani J, Kojima H, Ueda A, Kakizaki S, Yoshinari K, Gong QH, Owens IS, Negishi M, Sueyoshi T (2001) The phenobarbital response enhancer module in the human bilirubin UDP-glucuronosyltransferase UGT1A1 gene and regulation by the nuclear receptor CAR. *Hepatology* **33**: 1232-1238.

Sugatani J, Yamakawa K, Tonda E, Nishitani S, Yoshinari K, Degawa M, Abe I, Noguchi H, Miwa M (2004) The induction of human UDP-glucuronosyltransferase 1A1 mediated through a distal enhancer module by flavonoids and xenobiotics. *Biohem Pharmacol* **67**: 989-1000.

Sugatani J, Nishitani S, Yamakawa K, Yoshinari K, Sueyoshi T, Nagishi M, Miwa M (2005a) Transcriptional regulation of human UGT1A1 gene expression: Activated glucocorticoid receptor enhances constitutive androstane receptor/pregnane X receptor-mediated UDP-glucuronosyltransferase 1A1 regulation with glucocorticoid receptor-interacting protein 1. *Mol Pharmacol* **67**: 845-855.

Sugatani J, Sueyoshi T, Negishi M, Miwa M (2005b) Regulation of the human *UGT1A1* gene by nuclear receptors CAR, PXR and GR. In: Sies H, Packer L (eds) Conjugation Enzymes.

Methods in Enzymology, Elsevier, Philadelphia, pp.92-104.

Sugatani J, Mizushima K, Osabe M, Yamakawa K, Kakizaki S, Takagi H, Mori M, Ikari A, Miwa M (2008) Transcriptional regulation of human UGT1A1 gene expression through distal and proximal promoter motifs: implication of defects in the UGT1A1 gene promoter. *Naunyn-Schmiedeberg's Arch Pharmacol* **377**: 597-605.

Sugatani J, Osabe M, Kurosawa M, Kitamura N, Ikari A, Miwa M (2010) Induction of UGT1A1 and CYP2B6 by an antimitogenic factor in HepG2 cells is mediated through suppression of cyclin-dependent kinase 2 activity: Cell-cycle dependent expression. *Drug Metab Dispos* **38**: 177-186.

Timsit YE, N egishi M (2007) CAR and PXR: The xenobiotic-sensing receptors. *Steroid* **72**: 231-246.

Tukey RH, Strassburg CP (2000) Human UDP-glucuronosyltransferases: metabolism, expression, and disease. *Annu Rev Pharmacol Toxicol* **40**: 581-616.

Tukey RH, Strassburg CP, Mackenzie PI (2002) Pharmacogenomics of human UDP-glucuronosyltransferases and irinotecan toxicity. *Mol. Pharmacol.* **62**: 446-450.

Watkins RE, Davis-Searles PR, Lambert MH, Redinbo MR (2003) Coactivator binding promotes the specific interaction between ligand and the pregnane X receptor. *J Mol Biol* **331**: 815-828.

Wu Y, Shi X, Liu Y, Zhang X, Wang J, Luo X, Wen A (2012) Histone deacetylase 1 is required for carbamazepine-induced CYP3A4 expression. *J Pharm Biomed Anal* **58**: 78-82.

Yueh MF, Huang YH, Hiller A, Chen SJ, Nguyen N and Tukey RH (2003) Involvement of the xenobiotic response element (XRE) in Ah receptor-mediated induction of human UDP-glucuronosyltransferase 1A1. *J Biol Chem* **278**: 15001-15006.

Yueh MF and Tukey RH (2007) Nrf2-Keap1 signaling pathway regulates human UGT1A1 expression *in vitro* and in transgenic *UGT1* mice. *J Biol Chem* **282**: 8749-8756.

Footnote

This work was supported by the Global Center of Excellence Program from the Ministry of Education, Culture, Sports, Science and Technology, Japan; the Grant-in-Aid for Scientific Research from the Ministry of Education, Culture, Sports, Science and Technology, Japan [Grants 19590070, 19590151, 21590170, and 22590068].

DMD Fast Forward. Published on July 24, 2012 as DOI: 10.1124/dmd.112.046748
This article has not been copyedited and formatted. The final version may differ from this version.

Figure legends

Fig. 1 Effect of roscovitine on the transcriptional activities of the UGT1A1 distal (-3570/-3180) enhancer motif and proximal (-165/-1) promoter motif mediated by CAR, PXR, or AhR/ ARNT, assessed by expression of a reporter gene encoding firefly luciferase. HepG2 cells were cotransfected with expression plasmids for CAR (B), PXR (C, D), AhR/ARNT (E, F), or the control vector pCR3 (A), as well as the pGL4-tk-firefly luciferase vector reporter gene (open bar) or the *UGT1A1* reporter plasmid (closed bar). The transfected cells were treated with vehicle [dimethylsulfoxide (DMSO)] (C, E), 5 μM rifampicin (RIF) (D), 1 μM benzo[a]pyrene (B[a]P) (F) and then roscovitine at the indicated concentration for 24 h, harvested, and assayed for luciferase activity. Luciferase activity was measured using the dual-luciferase reporter assay system. Transcriptional activity of the *UGT1A1* reporter gene in the absence of roscovitine was calculated as one. Data presented are the average for three independent experiments ± S.E. * , $p < 0.05$; **, $p < 0.01$; ***, $p < 0.001$ roscovitine-treated *UGT1A1* reporter gene group versus vehicle-treated *UGT1A1* reporter gene group.

Fig. 2 Effect of roscovitine on expression of UGT1A1 and CYP3A4 in HepG2 cells expressing CAR or PXR. HepG2 cells cultured for 24 h were transfected with expression plasmids for CAR, CAR-ΔC8, PXR, and PXR-ΔC9 or the control vector pCR3. At 24 h a fter transfection, the medium was replaced, and the cells were further transfected, and then cultured with roscovitine (5 μM, closed bar) or vehicle (DMSO, open bar) for an additional 24 h. In A and B, the mRNA levels in cells transfected with pCR3 and treated with vehicle were taken as one. Data presented are the average ± S.E. for three experiments. ***$p < 0.001$ versus vehicle-treated cells; ###, $p < 0.001$ versus CAR or PXR-expressing cells. In C, protein levels were determined by Western blotting.

Fig. 3 T ransactivation capacity of *UGT1A1* (A) and *CYP3A4* (B) by phosphomimetic mutant

PXR proteins. HepG2 cells cultured for 24 h were transfected with expression vectors encoding wild-type or mutant PXR or the control vector pCR3. At 24 h after transfection, the medium was replaced, and the cells were further transfected, and then cultured with roscovitine (5 μM, closed bar), rifampicin (5 μM, hatched bar) or vehicle (DMSO, open bar) for an additional 24 h. The mRNA levels are expressed by taking the control value obtained from the pCR3-transfected and vehicle-treated cells as one. Data presented are the average ± S.E. of 4 – 11. *, $p<0.05$, **, $p<0.01$, ***, $p<0.01$ versus rifampicin-stimulated wild-type PXR; #, $p<0.05$, ##, $p<0.01$, ###, $p<0.01$ versus roscovitine-stimulated wild-type PXR.

Fig. 4 Relative transactivation capacity of *UGT1A1* by phosphodeficient (A, C) and phosphomimetic (B, D) mutant PXR. HepG2 cells cultured for 24 h were transfected with expression vectors encoding wild-type or mutant PXR or the control vector pCR3. At 24 h after transfection, the medium was replaced, and the cells were further transfected, and then cultured with roscovitine (5 μM) (A, B), rifampicin (5 μM) (C, D) or vehicle (DMSO) for an additional 24 h. The UGT1A1 mRNA levels are expressed by taking the value obtained from the wild-type PXR expression vector-transfected and roscovitine-treated cells as one. Data presented are the average ± S.E. of 4 – 11. *, $p<0.05$, **, $p<0.01$, ***, $p<0.01$ versus rifampicin-stimulated wild-type PXR; #, $p<0.05$, ##, $p<0.01$, ###, $p<0.01$ versus roscovitine-stimulated wild-type PXR.

Fig. 5 Stability of CYP3A4 and UGT1A1 mRNAs. HepG2 cells cultured for 48 h were treated with vehicle (DMSO) (A) or roscovitine (5 μM) (B) for an additional 24 h and then actinomycin D (2 μg) was added to block translation. CYP3A4 and UGT1A1 mRNA levels remaining after addition of actinomycin D were determined. The mRNA levels at time 0 (CYP3A4, 2.90 $\pm$ 0.21 fold induction; UGT1A1, 6.31 $\pm$ 0.16 fold induction) are expressed as one. Data presented are the average ± S.E. for three experiments. *$p<0.05$,

CYP3A4 mRNA levels versus UGT1A1 mRNA levels.

Fig. 6 Effect of anti-CDK1, anti-CDK2, and anti-CDK5 siRNA transfection on expression of UGT1A1 mRNA and phosphorylation of PXR at S350 by CDK2. In A, SW480 cells cultured for 24 h were transfected with anti-CDK siRNA (100 nM) or mock-transfected. At 24 h after transfection, the medium was replaced, and the cells were further transfected with anti-CDK siRNA (100 nM) or mock-transfected, and then cultured for an additional 24 h. The mRNA levels in cells cultured for 48 h (control group) were taken as one. Data presented are the average ± S.E. for three experiments. $^{**}p<0.01$; $^{***}p < 0.001$ versus the mock-transfected group. In B, whole-cell lysate was prepared from SW480 cells at 2 h after release from the thymidine block and immunoprecipitated (IP) with anti-CDK2 antibody. Immune complex kinase assays were performed using GST-fused forms of wild-type and S350D mutant PXR as substrates. Experiments were done twice with similar results, and representative data are shown.

Fig. 7 Western blot analysis of expressed PXR constructs fused with YFP in HepG2 cells. HepG2 cells cultured for 24 h were transfected with constructs expressing the wild-type and mutant YFP-PXR fusion proteins. At 24 h after transfection, the medium was replaced, and the cells were further transfected, and then cultured with roscovitine (5 μM) or vehicle (DMSO) in the absence (A, B, C) or presence (C) of MG-132 (5 μM) for an additional 24 h. The nuclear (A) and cytoplasmic (B, C) YFP-PXR proteins were determined by Western blotting with the indicated antibodies.

Fig. 8 Subcellular localization of expressed PXR constructs fused with YFP in HepG2 cells. HepG2 cells cultured for 24 h were transfected with constructs expressing the wild-type and mutant YFP-PXR fusion proteins. At 24 h after transfection, the medium was replaced, and the cells were further transfected, and then cultured with roscovitine (5 μM) or vehicle (DMSO) for an additional 24 h. The subcellular localization of the YFP-PXR protein was observed by fluorescence microscopy.

Fig. 9 SRC-2 is a critical transcriptional co-activator for S350D mutant PXR in HepG2 cells. HepG2 cells cultured for 24 h were transfected with constructs expressing wild-type or mutant PXR protein and SRC-1 or SRC-2 protein. At 24 h after transfection, the medium was replaced, and the cells were further transfected, and then cultured with roscovitine (5 μM) or vehicle (DMSO) for an additional 24 h. The mRNA levels of UGT1A1 are expressed by taking the control value obtained from the control vector pCR3- and pcDNA3.1-transfected and vehicle-treated cells as one. Data presented are the average ± S.E. for three experiments. a, $p<0.001$ wild-type PXR versus S350D mutant PXR; b, $p<0.05$ S350D mutant PXR versus S350D mutant PXR plus SRC-2.

Fig. 10 Binding of wild-type or mutant YFP-PXR fusion protein to cytoplasmic HSP90 and CCRP (A) and to nuclear RXR, HDAC1, and HDAC3 (B) and acetylation of wild-type or mutant protein (B). HepG2 cells cultured for 24 h were transfected with constructs expressing wild-type and mutant YFP-PXR fusion proteins. At 24 h after transfection, the medium was replaced, and the cells were further transfected, and then cultured with roscovitine (5 μM) or vehicle (DMSO) for an additional 24 h. Cytoplasmic fractions and nuclear extracts were prepared and used for immunoprecipitation (IP) using anti-GFP antibody or anti-CCRP antibody and Western blotting stained with the indicated antibodies.

DMD Fast Forward. Published on July 24, 2012 as DOI: 10.1124/dmd.112.046748
This article has not been copyedited and formatted. The final version may differ from this version.

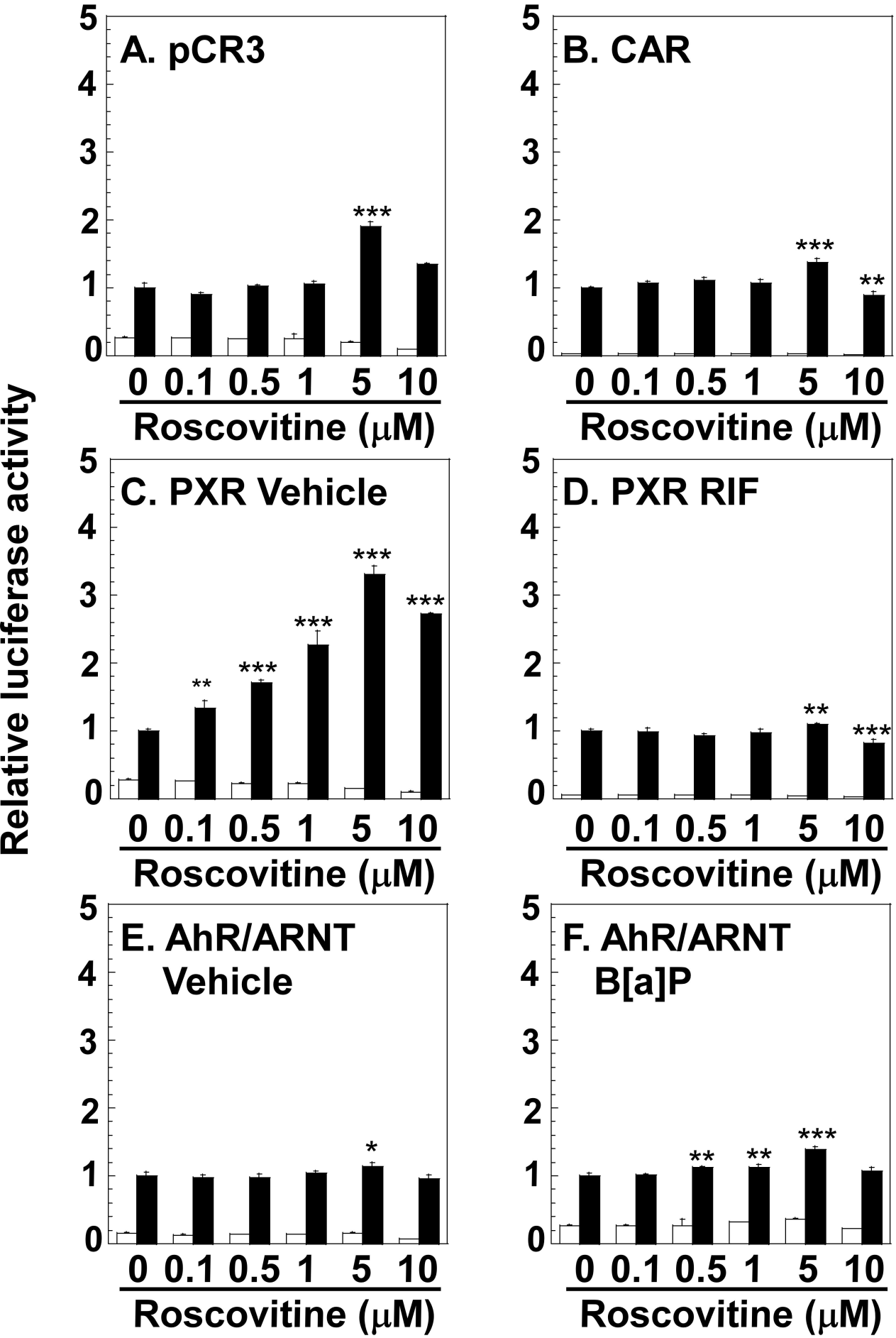

Fig. 1

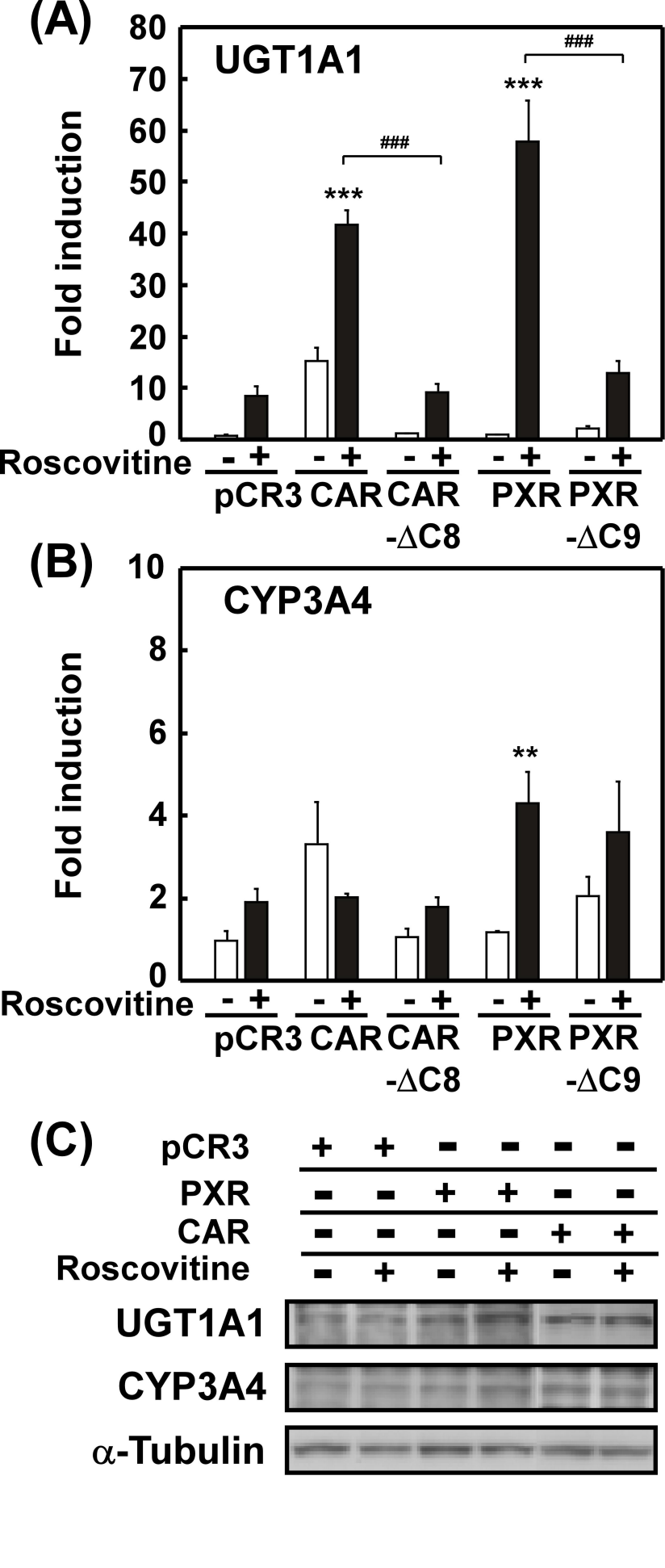
(A)
UGT1A1
Fold induction
80
70
60
50
40
30
20
10
0
***
###
***
###
Roscovitine
- + - + - + - + - +
pCR3
CAR
CAR -ΔC8
PXR
PXR -ΔC9
(B)
CYP3A4
Fold induction
10
8
6
4
2
0
**
Roscovitine
- + - + - + - + - +
pCR3
CAR
CAR -ΔC8
PXR
PXR -ΔC9
(C)
pCR3 + + - - - -
PXR - - + + - -
CAR - - - - + +
Roscovitine - + - + - +
UGT1A1
CYP3A4
α-Tubulin

Fig. 2

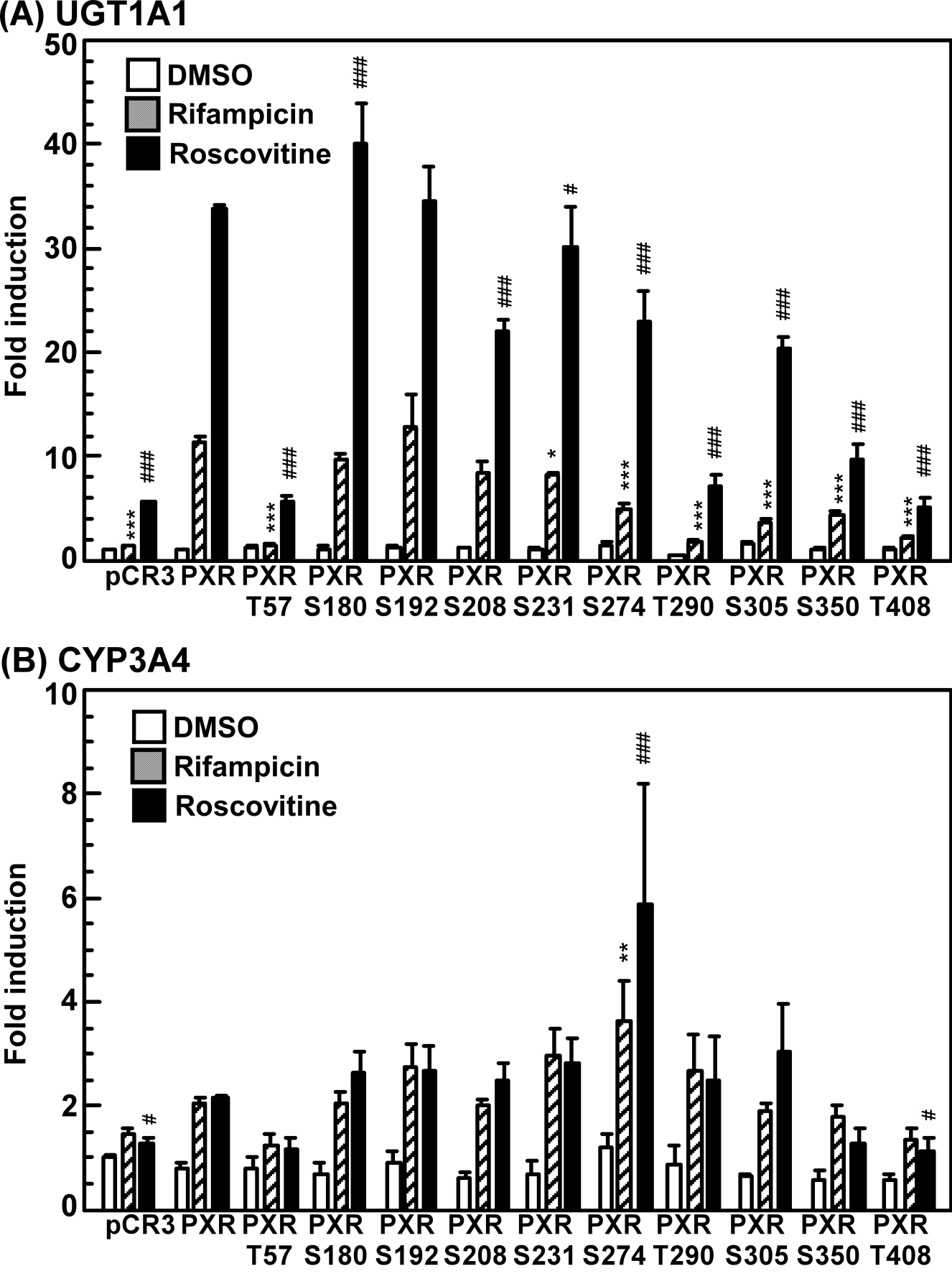
(A) UGT1A1
DMSO
Rifampicin
Roscovitine
Fold induction
50
40
30
20
10
0
pCR3
PXR
PXR T57
PXR S180
PXR S192
PXR S208
PXR S231
PXR S274
PXR T290
PXR S305
PXR S350
PXR T408
(B) CYP3A4
DMSO
Rifampicin
Roscovitine
Fold induction
10
8
6
4
2
0
pCR3
PXR
PXR T57
PXR S180
PXR S192
PXR S208
PXR S231
PXR S274
PXR T290
PXR S305
PXR S350
PXR T408

Fig. 3

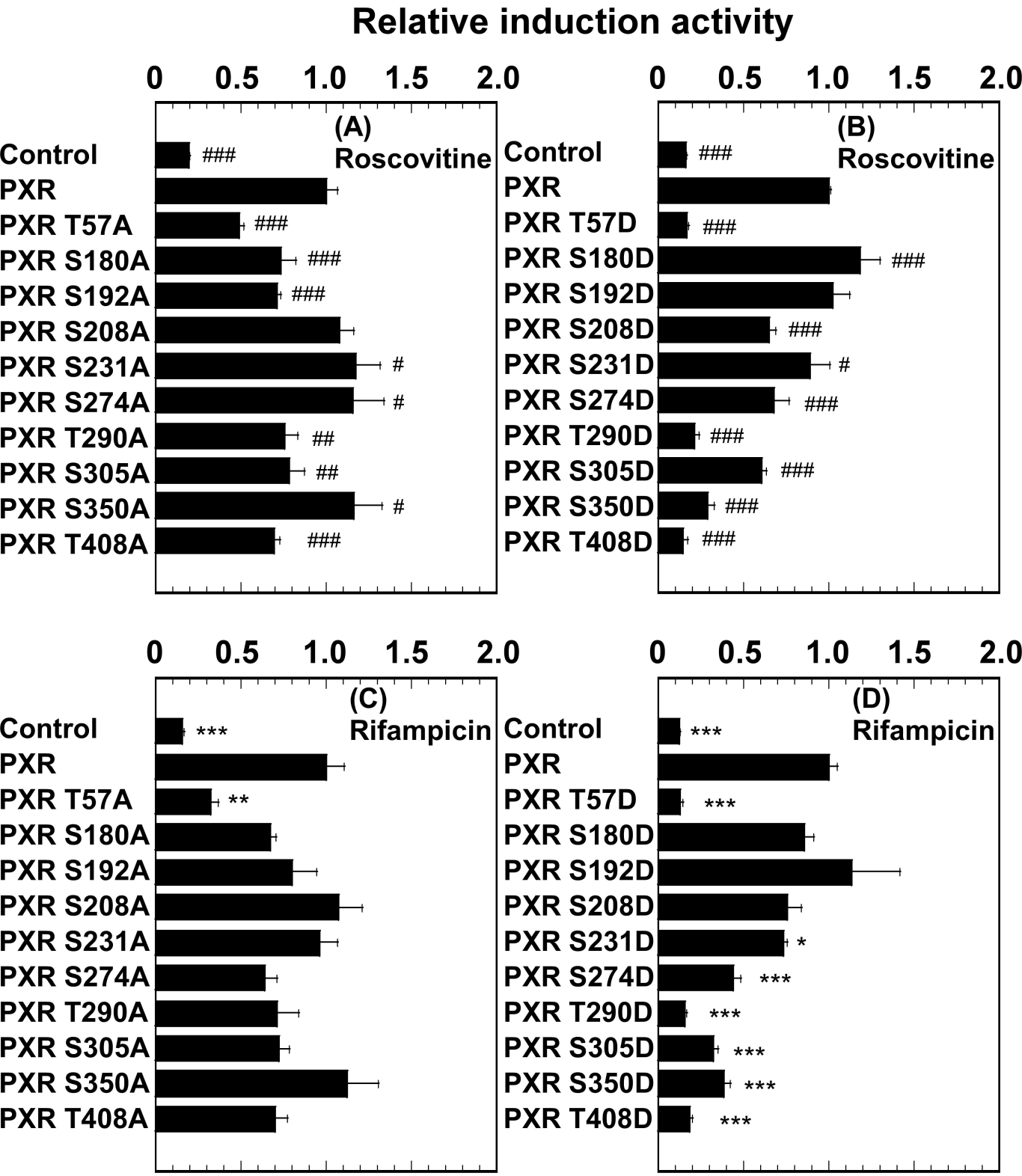
Relative induction activity
0
0.5
1.0
1.5
2.0
(A)
Roscovitine
Control
PXR
PXR T57A
PXR S180A
PXR S192A
PXR S208A
PXR S231A
PXR S274A
PXR T290A
PXR S305A
PXR S350A
PXR T408A
###
###
###
###
#
#
##
##
#
###
(B)
Roscovitine
Control
PXR
PXR T57D
PXR S180D
PXR S192D
PXR S208D
PXR S231D
PXR S274D
PXR T290D
PXR S305D
PXR S350D
PXR T408D
###
###
###
###
#
###
###
###
###
###
(C)
Rifampicin
Control
PXR
PXR T57A
PXR S180A
PXR S192A
PXR S208A
PXR S231A
PXR S274A
PXR T290A
PXR S305A
PXR S350A
PXR T408A
***
**
(D)
Rifampicin
Control
PXR
PXR T57D
PXR S180D
PXR S192D
PXR S208D
PXR S231D
PXR S274D
PXR T290D
PXR S305D
PXR S350D
PXR T408D
***
***
*
***
***
***
***
***

Fig. 4

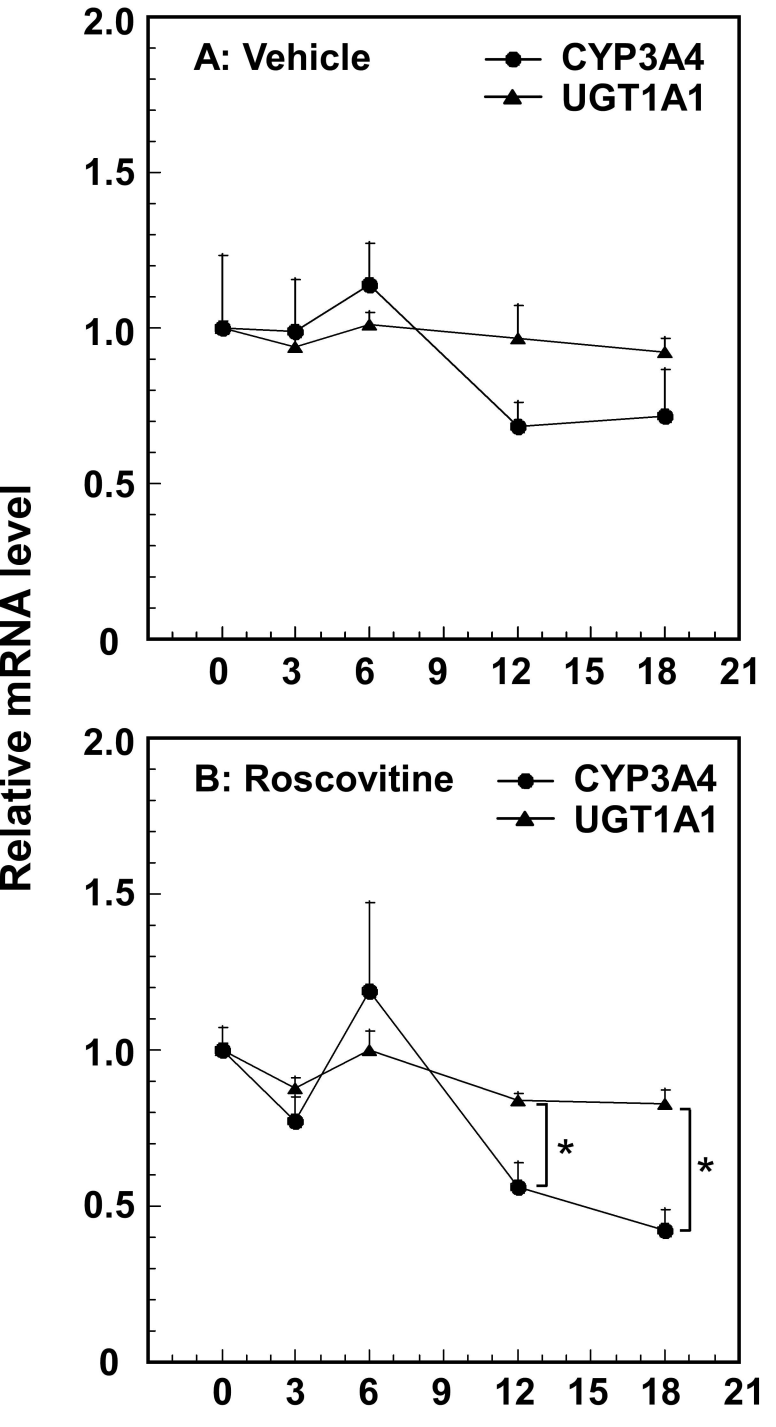
A: Vehicle
CYP3A4
UGT1A1
B: Roscovitine
CYP3A4
UGT1A1
Relative mRNA level
2.0
1.5
1.0
0.5
0
0
3
6
9
12
15
18
21
*
*
Time after actinomycin D treatment (h)

Fig. 5

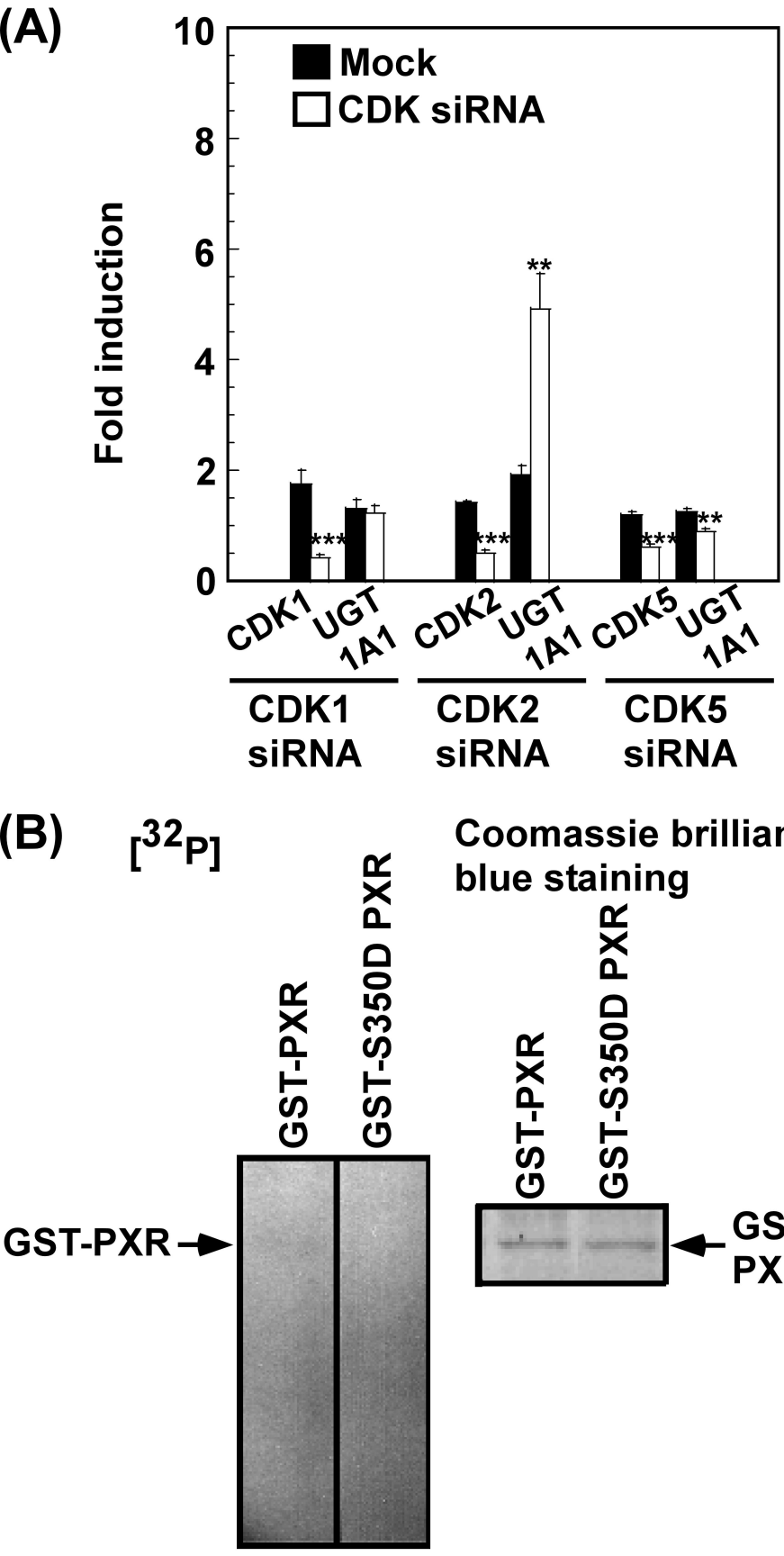
(A)
Mock
CDK siRNA
Fold induction
10
8
6
4
2
0
**
***
***
**
***
**
CDK1
UGT 1A1
CDK2
UGT 1A1
CDK5
UGT 1A1
CDK1 siRNA
CDK2 siRNA
CDK5 siRNA
(B)
[32P]
Coomassie brilliant blue staining
GST-PXR
GST-S350D PXR
GST-PXR
GST-PXR
GST-S350D PXR
GST-PXR

Fig. 6

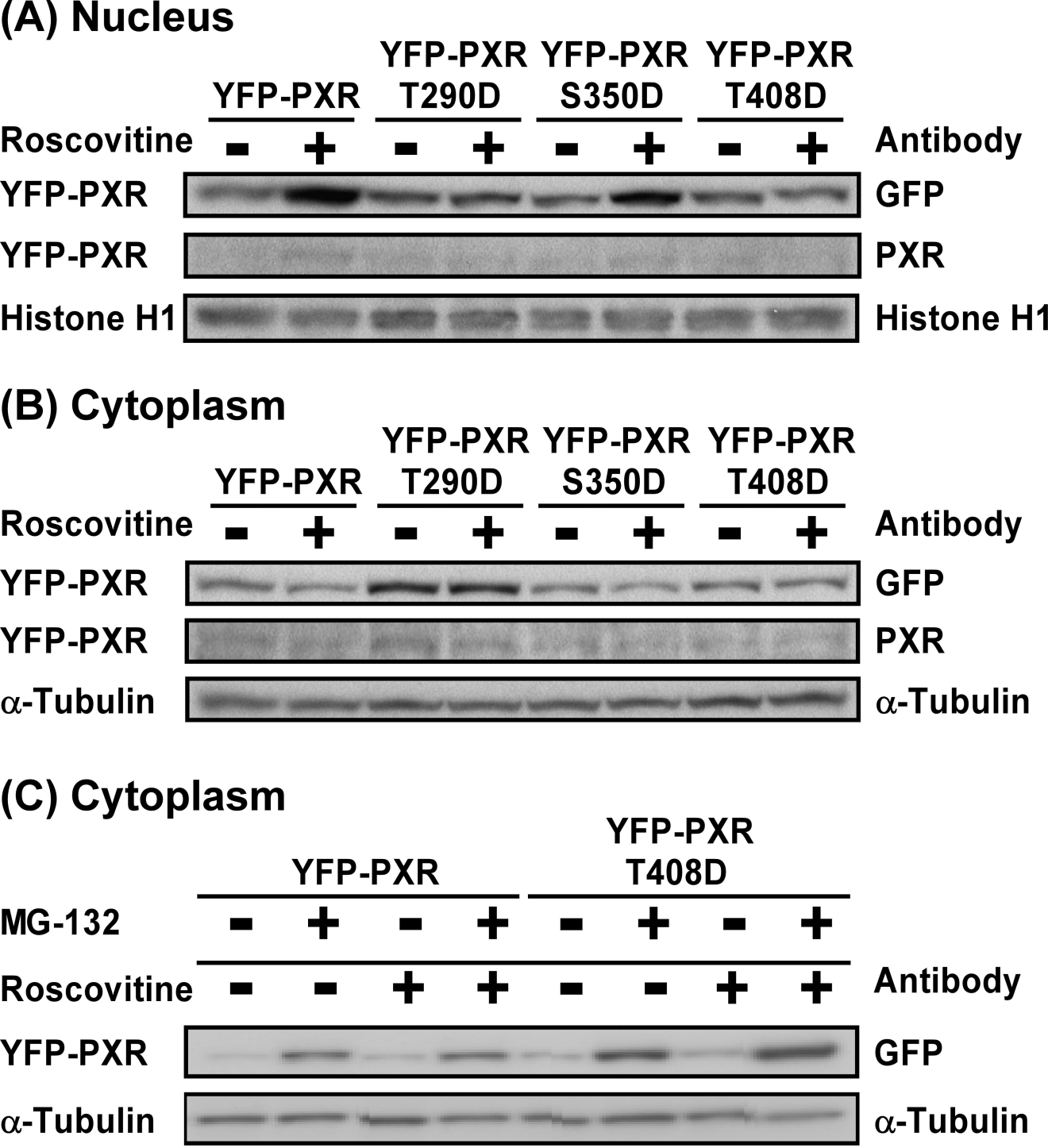
(A) Nucleus
YFP-PXR
YFP-PXR T290D
YFP-PXR S350D
YFP-PXR T408D
Roscovitine
Antibody
YFP-PXR
GFP
YFP-PXR
PXR
Histone H1
Histone H1
(B) Cytoplasm
YFP-PXR
YFP-PXR T290D
YFP-PXR S350D
YFP-PXR T408D
Roscovitine
Antibody
YFP-PXR
GFP
YFP-PXR
PXR
α-Tubulin
α-Tubulin
(C) Cytoplasm
YFP-PXR
YFP-PXR T408D
MG-132
Roscovitine
Antibody
YFP-PXR
GFP
α-Tubulin
α-Tubulin

Fig. 7

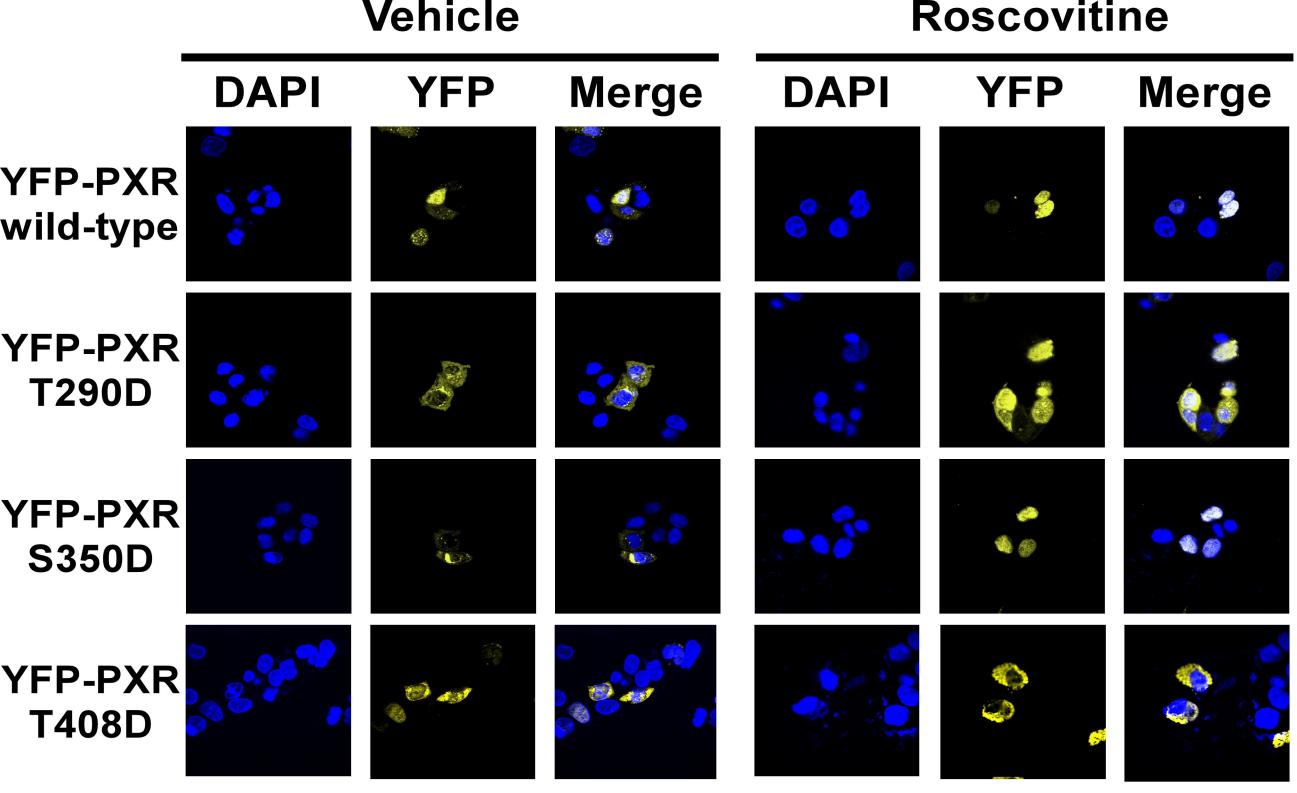
Vehicle
Roscovitine
DAPI
YFP
Merge
DAPI
YFP
Merge
YFP-PXR wild-type
YFP-PXR T290D
YFP-PXR S350D
YFP-PXR T408D

Fig. 8

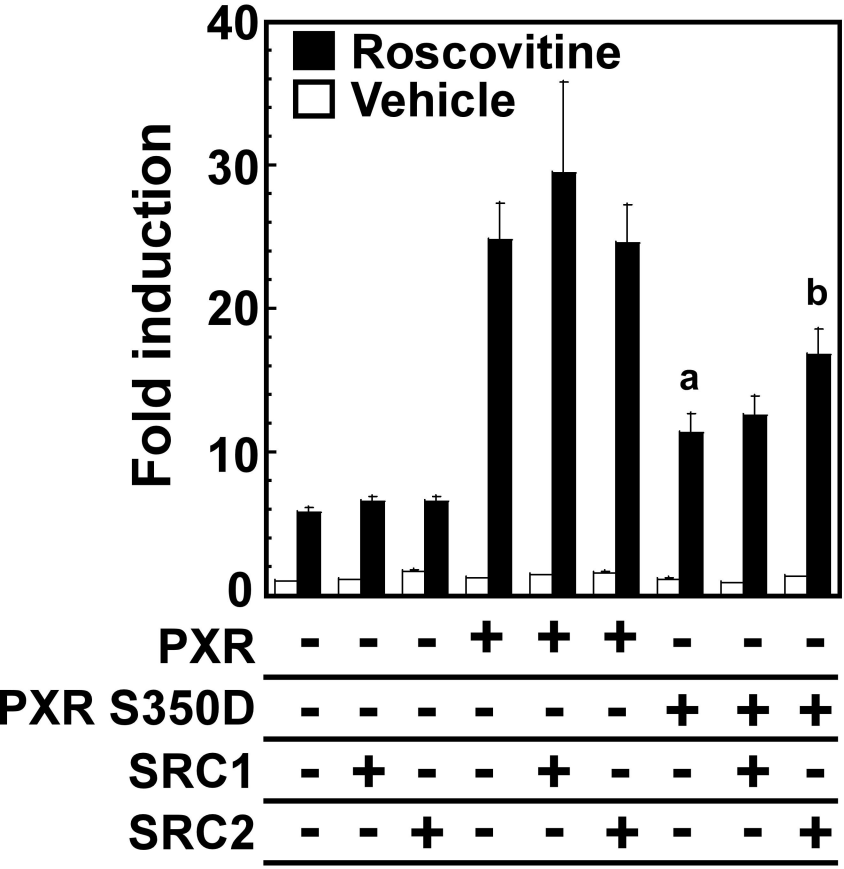
Roscovitine
Vehicle
Fold induction
40
30
20
10
0
a
b
PXR - - - + + + - - -
PXR S350D - - - - - - + + +
SRC1 - + - - + - - + -
SRC2 - - + - - + - - +

Fig. 9

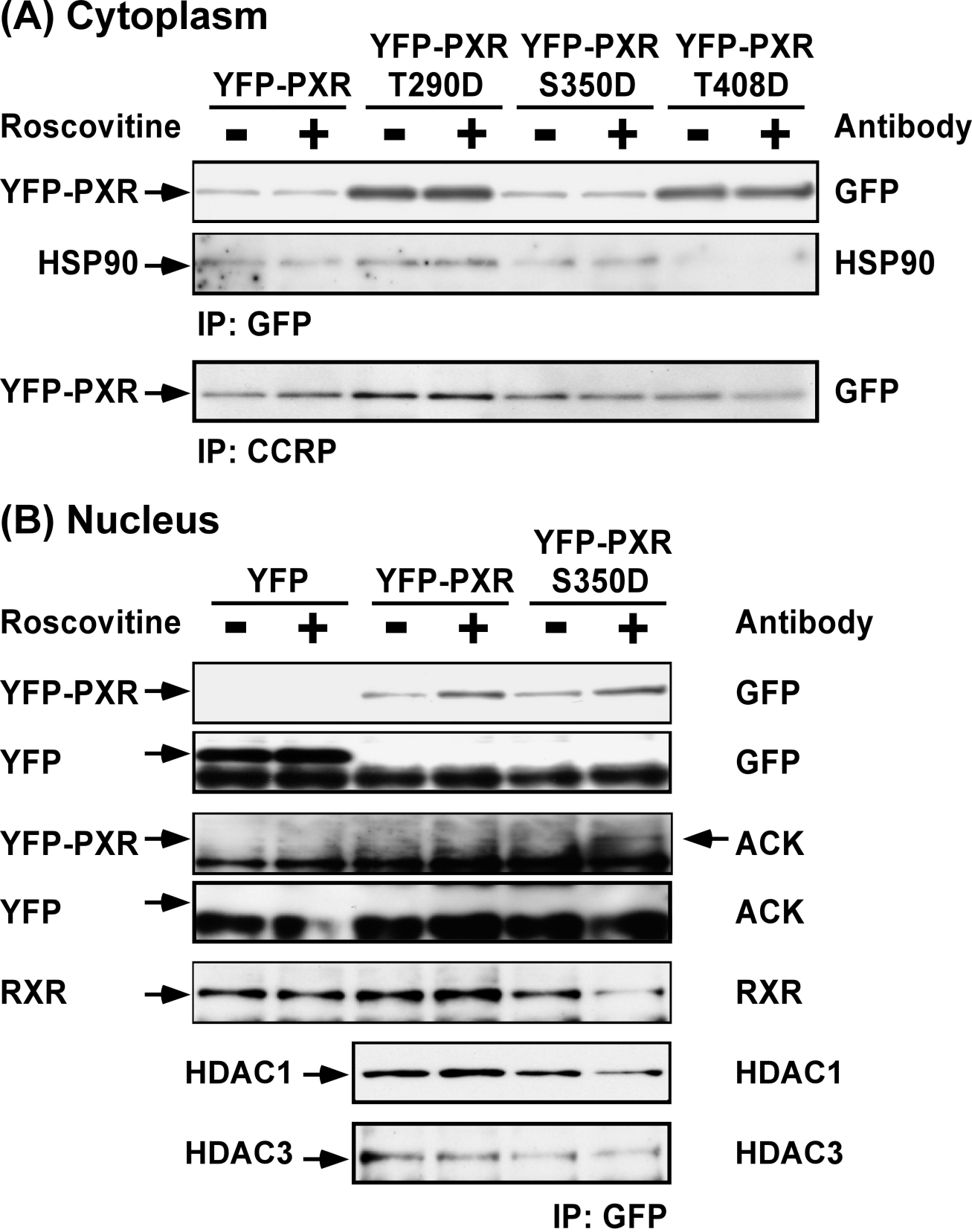
(A) Cytoplasm
YFP-PXR
YFP-PXR T290D
YFP-PXR S350D
YFP-PXR T408D
Roscovitine
- + - + - + - +
Antibody
YFP-PXR
GFP
HSP90
HSP90
IP: GFP
YFP-PXR
GFP
IP: CCRP
(B) Nucleus
YFP
YFP-PXR
YFP-PXR S350D
Roscovitine
- + - + - +
Antibody
YFP-PXR
GFP
YFP
GFP
YFP-PXR
ACK
YFP
ACK
RXR
RXR
HDAC1
HDAC1
HDAC3
HDAC3
IP: GFP

Fig. 10